Single crystallites in "planar polycrystalline" oligothiophene films

Vrijmoeth, J.; Stok, R. W.; Veldman, R.; Schoonveld, W. A.; Klapwijk, T. M.

Published in:
Journal of Applied Physics

DOI:
10.1063/1.367145

Publication date:
1998

Single crystallites in “planar polycrystalline” oligothiophene films: Determination of orientation and thickness by polarization microscopy

J. Vrijmoeth, R. W. Stok, R. Veldman, W. A. Schoonveld, and T. M. Klapwijk

Citation: Journal of Applied Physics **83**, 3816 (1998); doi: 10.1063/1.367145
View online: https://doi.org/10.1063/1.367145
View Table of Contents: http://aip.scitation.org/toc/jap/83/7
Published by the American Institute of Physics

Single crystallites in "planar polycrystalline" oligothiophene films: Determination of orientation and thickness by polarization microscopy

J. Vrijmoeth,[a] R. W. Stok, R. Veldman, W. A. Schoonveld, and T. M. Klapwijk
Department of Applied Physics and Materials Science Center, University of Groningen, Nijenborgh 4, 9747 AG Groningen, The Netherlands

(Received 11 September 1997; accepted for publication 19 December 1997)

Thin films of evaporated oligothiophenes (α-nT, $n=4-8$) show a "planar polycrystalline" structure: each of the individual crystallites has a random azimuthal orientation, the (a,b) face of its unit cell is aligned with the surface plane. We introduce a technique to determine the orientation and thickness of such aligned thiophene crystals by optical polarization microscopy. Due to the optical birefringence of the crystal, it appears with different colors in the microscope dependent on its orientation and thickness. To support the method proposed, we solve Maxwell's equations and obtain quantitative agreement with the observed colors. The organic crystal shows biaxial anisotropy. For unsubstituted quaterthiophene, α-$4T$, we find effective refractive indices $n_b = 1.84 \pm 0.1$ and $n_a = 1.61 \pm 0.1$ for waves under normal incidence. Our conclusions are fully confirmed by atomic force microscopy with molecular resolution. Our analyses result in a simple recipe to obtain the directions of the *a* and *b* crystal axes from the optical experiment. © *1998 American Institute of Physics.* [S0021-8979(98)02007-6]

I. INTRODUCTION

Following the pioneering work by Horowitz *et al.*,[1] field-effect transistors based on evaporated oligothiophenes (α-nT, $n=4-8$ monomer units) have been intensively studied.[2,3] Their special crystalline order makes these materials well suited for the study of the intrinsic charge transport properties of organic solids.[2,4,5] Under suitable preparation conditions the thiophene material crystallizes with its (a,b) crystal face aligned with the substrate plane; its molecules are almost perpendicular to the surface. This induces a "planar polycrystalline" order in the film. Each of the crystallites has its *a* and *b* axes residing within the surface plane, but has a different azimuthal orientation.

Ideally, one would like to perform the study of field-effect charge transport on such a single organic crystal. It would allow to analyze the transport along both in-plane crystal axes. Further, it would rule out the influence of grain boundaries. Until now, the films prepared by vacuum evaporation have had grain sizes smaller than $\sim 0.2\ \mu$m.[6] It was only on the basis of a bulk-grown crystal that a single-crystal device has been realized.[7] Recently, however, we have obtained large single crystallites with diameters up to $\sim 25\ \mu$m of both quaterthiophene and sexithiophene by vacuum evaporation and realized transistors with such a single crystal in the active region.[8] To measure the mobilities along each of the crystal axes in the surface plane, one then must know their azimuthal directions.

In this article, we introduce a simple and reliable technique to determine the directions of both in-plane crystal axes in each individual thiophene crystal by polarization microscopy.[9,10] Optical crystallography has been developed into a useful technique for the study of oriented layers,[11] especially of Langmuir Blodgett films.[12]

Because of their optical birefringence, the individual crystals appear with a strong color contrast in the microscope for different azimuthal orientations. We calculate the reflectivities solving Maxwell's equations for plane waves in the anisotropic medium. The calculations are in excellent agreement with the observed colors. The data are properly described assuming that the crystal shows biaxial anisotropy.

As a result of our work, we find a simple recipe to obtain the crystal axis directions. The thickness of the crystallite is obtained as a side product. The directions of the *a* and *b* crystal axes as obtained from the microscope coincide with those found by atomic force microscopy (AFM).

We believe that our method is generally applicable to obtain the in-plane crystal orientation of birefringent materials showing the present planar polycrystalline surface ordering mode. This mode is commonly found for various materials on planar substrates, both amorphous and crystalline.

II. EXPERIMENT

Thin quaterthiophene films have been deposited on oxidized Si(100) substrates. The thermally grown oxide layer had a thickness in the range of 120–160 nm, as determined by ellipsometry. The organic films were grown by thermal evaporation from a small Ta boat in high vacuum (background pressure 10^{-7} mbar). Because of the significant desorption of the evaporant from the surface that occurs at the evaporation substrate temperature ($\sim 70\ ^\circ$C), the substrate was forced to cool down rapidly to room temperature (rate $\sim 3.5\ ^\circ$C per min) immediately following the evaporation. Further analyses were performed after the sample had been removed from the vacuum.

[a]Electronic mail: j.vrymoeth@phys.rug.nl

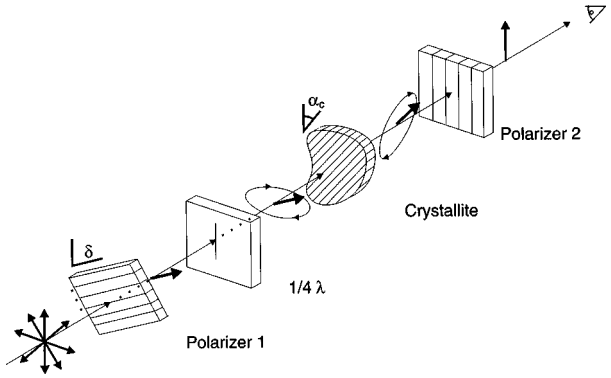

FIG. 1. Setup of the polarizing elements in the microscope. The optical path is represented as a straight line for clarity. Linearly or circularly polarized light is incident on the crystallite through a polarizer, with angle δ, and a $\lambda/4$ retarder plate. The reflected light is analyzed by a vertical linear polarizer. The angles δ and α_c of the polarizer and crystallite are defined with respect to the vertical axis, both in this figure and in the optical images.

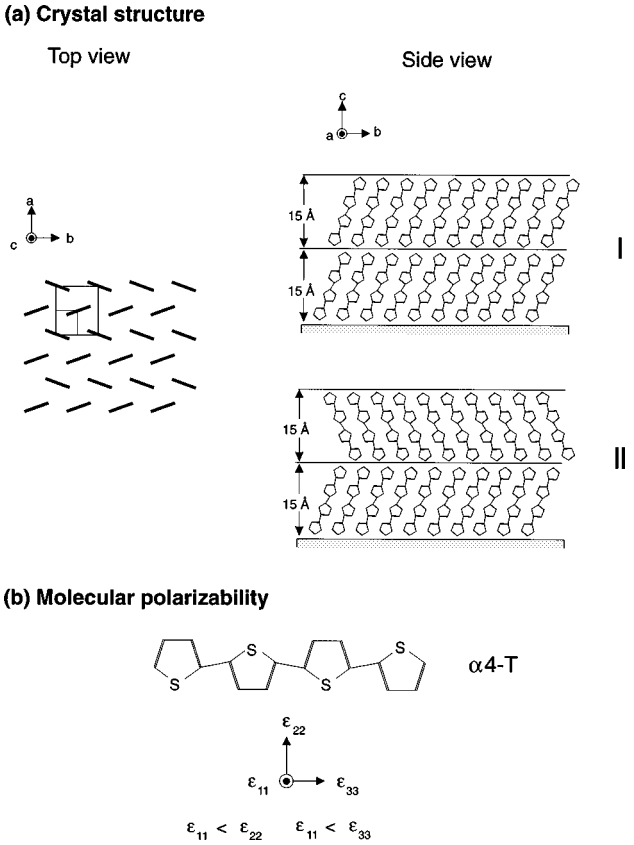

FIG. 2. (a) Possible crystal structures of evaporated quaterthiophenes consistent with the layering found from $\Theta-2\Theta$ x-ray data on evaporated films. (I) has been proposed on the basis of powder diffraction data [Porzio1], (II) is the structure which has been proposed for α-3T [Bolhuis1] and dimethyl-substituted quaterthiophene[Hotta1]. (b) Polarizability of a single α-4T molecule. The polarizability $\epsilon_{\text{crystal}}$ of the crystal is approximated by taking the average of the molecular polarizabilities in the unit cell.

Average film thicknesses were determined using a Dektak surface profiler. AFM images were taken in air using a commercial instrument (Park Scientific) in contact mode.

The optical data were taken in reflection mode using a commercial high-resolution polarization microscope (Olympus BH-2). The arrangement of the polarizing elements in the optical path is sketched in Fig. 1 and is represented along a straight line for clarity. Angles are defined with respect to the vertical axis. Noncoherent white light with either linear or circular polarization is incident on the sample through a rotatable linear polarizer (rotation angle δ) and a $\lambda/4$ retarder plate. The sample is mounted in the microscope on a rotatable stage so that its angle of rotation α_{sample}, and that of each of the crystallites, α_c, can be varied. α_c is chosen to be the angle of the b crystal axis with respect to the vertical direction (see Fig. 2). The reflected light was analyzed with a linear polarizer.

With this setup, the polarization of the incident light can be chosen to be vertical ($\delta=0°$), circular ($\delta=45°$) or horizontal ($\delta=90°$). Due to the beam splitter which separates the entrance and exit beams, the optical transmission of the microscope appears to be different for horizontally and vertically polarized light. This partial polarization has been checked to be essentially independent of wavelength, and has been taken into account in the calculations (see Sec. IV B). The optical images were recorded using a CCD color video camera and digitized to obtain the R, G, and B color components.

III. FILM STRUCTURE: ''PLANAR POLYCRYSTALLINE''

The special planar polycrystalline ordering of the α-4T film is illustrated in Figs. 2 and 3. X-ray Θ-2Θ scans reproducibly reveal an ensemble of very sharp peaks (not shown), corresponding to a layering in the z direction with 1.58 nm periodicity [Fig. 2(a). In addition we have resolved terraces and steps with the same height using AFM (not shown).] We observe this behavior consistently for substrate temperatures between 20 and 120 °C.[13]

The polycrystallinity of the film, with each of the oriented crystallites in a random azimuthal orientation, is evident in the microscope (Fig. 3). (We find that the sizes of the individual single crystals critically depend on the preparation conditions and can become very large (diameter $\sim 25\ \mu$m) for optimized substrate temperatures and evaporation rates.[14])

This ordering behavior is generally found for the thiophene materials,[6,15,16] with the (a,b) crystal face aligned with the surface plane, and the molecules in a herringbone arrangement. The oligomer is oriented with its molecules almost perpendicular to the substrate plane [see Fig. 2(a)]. The detailed molecular structures occurring may show variations for the different materials.

We note that the data for quaterthiophene are however consistent with two different microstructures I and II [see Fig. 2(a)]. Either the tilt direction of the molecules is the same for each successive layer (I), or it changes over 180° azimuth for every next thiophene layer (II). Model I is supported by diffraction studies on quaterthiophene powder.[15] Structure II was found both for end-capped quaterthiophene,[17] and for terthiophene.[18] These different structures also imply different optical symmetries of the

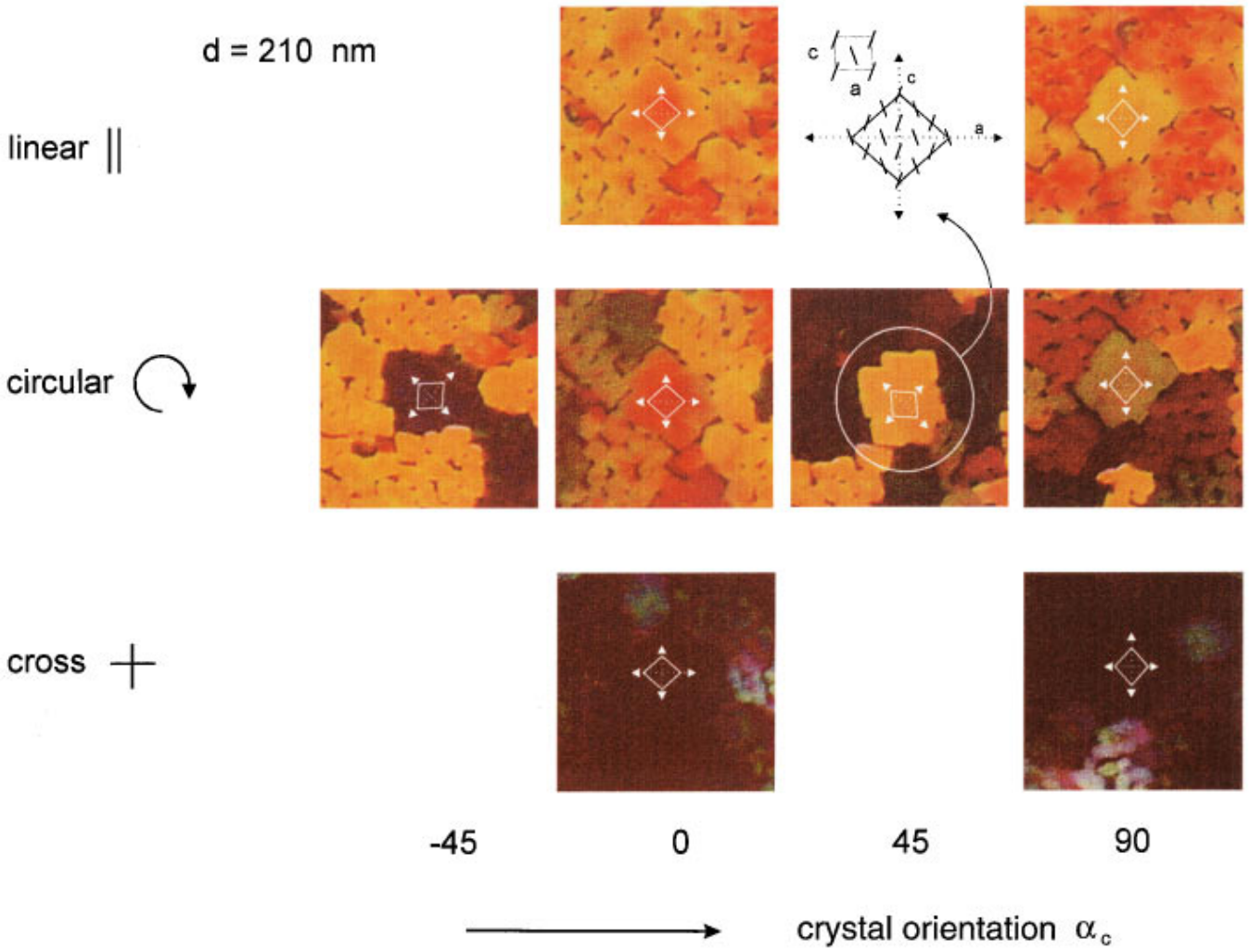

FIG. 3. (Color) Appearance in the optical microscope of a single crystallite (thickness ~210 nm), for different polarization states of the incident light and crystallite orientations α_c. The numbers α_c refer to the crystallite in the circle. The maximum reflected intensity for circularly polarized light is observed at $\alpha_c \sim 45°$.

crystal. On the basis of its optical behavior, we can therefore distinguish these structures (Appendix C).

IV. OPTICAL APPEARANCE OF THE INDIVIDUAL CRYSTALLITES

A. Observation

The individual crystallites show large variations in color in the microscope (see Fig. 3) for different light polarization states, thicknesses, and azimuthal orientations. These variations in color can therefore be employed to obtain the individual orientations. We discuss these colors for different relative angles δ of the entrance and exit polarizers.

$\delta = 0°$. Figure 3 shows two optical micrographs taken for $\delta = 0°$ with parallel polarizers from a film area with a measured thickness of ~210 nm. Depending on its orientation in the microscope, each of the crystallites in this film appears with a specific color (between green/yellow and red for this thickness). We will show below that these colors occur when the *b* or the *a* base vector in the unit cell coincides with the vertical analyzer polarization, i.e., for $\alpha_c = 0°$ and $\alpha_c = 90°$.

$\delta = 45°$. With circularly polarized light incident on the sample, the overall color appearance of the film changes drastically, with an enhanced contrast. Now one bright maximum per 180° rotation is observed (Fig. 3, middle row). Interestingly, this maximum in intensity (yellow/white color in middle row) does not occur for $\alpha_c = 0°$ or $\alpha_c = 90°$, but for $\alpha_c \sim 45°$, independent of crystallite thickness. The absolute color, however, varies with thickness.

$\delta = 90°$. If the incident polarizer is crossed with respect to the analyzer, the reflected intensity almost vanishes (Fig. 3, bottom). Some light is observed for $\alpha_c = 45°$. The intensity is zero for $\alpha_c = 0°$ and $\alpha_c = 90°$, i.e., if the polarizer and analyzer coincide with either the *b* or the *a* axis of the unit cell. This phenomenon can be employed to align the crystal accurately with the polarizers, to within ~3°, by minimization of the reflected intensity.

These findings can be used to develop a straightforward recipe to identify the crystal axes from the observed color extrema. We have modeled the optical reflectance of the sample to support such a recipe.

B. Model calculation

We describe these observations in terms of the interference between light waves reflected from the crystallite surface and those from the crystallite-substrate interface. The wavelength of the light depends on its polarization direction, and this gives rise to the differences in interference color.

We have calculated the reflectance of the thiophene-SiO_2-Si layered thin-film system to find its colors either in the optical microscope, or as seen by the bare eye over macroscopic film areas. In the former case, we assume that the light wave is incident under a cone of angles (numerical aperture of the objective 0.9) centered around the surface normal; in the latter the light is incident along the surface normal only.

The description of the sample reflection for both the *s*-and the *p*-polarization states (Jones matrix) requires the solution of Maxwell's equations in each of the layers of the sample. (The permittivity of the thiophene film is characterized by an anisotropic tensor ϵ.[19]) To that end, we have followed the approach developed by Berreman *et al.*[20] The propagation of the plane waves in the z direction, i.e., perpendicular to the interface, is described by a vector $\Psi(z) = (E_x, H_y, E_y, -H_x)$, which contains the tangential magnetic and electric field components. Within this formulation, the wave equations reduce to $d\Psi/dz = (i\omega/c)\Delta \cdot \Psi$. Here, Δ is the (4×4) so-called layer propagation matrix, which contains the permittivity tensor ϵ and is different for each angle of incidence. The solution to Maxwell's equations takes the form $\Psi(z) = \exp[(i\omega z/c)\Delta]\cdot\Psi(0)$. Hence the wave fields at the respective interfaces, as described by $\Psi(0)$ and $\Psi(d)$, are related by

$$\Psi(d) = \exp\left(\frac{i\omega d}{c}\,\Delta\right)\cdot\Psi(0), \tag{1}$$

with d the crystallite thickness. The (4×4) ''layer matrix'' $\exp[(i\omega d/c)\Delta]$ is obtained from Δ by diagonalization. The four eigenvectors of Δ represent the four wave solutions that can occur in the anisotropic medium.[10] The eigenvalues are the effective refractive indices for these waves. This procedure effectively results in decomposing the incident wave field in terms of these four eigenwaves.[20] The reflectivities and transmissivities of the sample are finally obtained by matching the incident, reflected and transmitted waves at each interface, as in the standard Fresnel approach.[20,21]

We have applied this method to the quaterthiophene single crystal. Its polarizability tensor $\epsilon_{\text{crystal}}$ was constructed assuming that it can be approximated by averaging the contributions of the different molecules within the unit cell. The main polarizabilities $(\epsilon_{\text{mol}})_{ii}$, $(i=1,2,3)$ of the α-$4T$ molecules [see Fig. 2(b)] were assumed large within the molecular plane and small perpendicular to it $[(\epsilon_{\text{mol}})_{22} \approx (\epsilon_{\text{mol}})_{33}$, $(\epsilon_{\text{mol}})_{22,33} > (\epsilon_{\text{mol}})_{11}]$. The thiophene polarizabilities were assumed to be independent of wavelength. $\epsilon_{\text{crystal}}$ for each of the models I and II was constructed by placing the molecules within the unit cell and averaging their contributions to the total tensor. Note that with this approach the influence of the local field[12] is neglected.

The reflectivities and transmissivities of the SiO_2/Si interface were described by standard Fresnel coefficients. The refractive indices for Si and SiO_2 as a function of wavelength have been taken from Refs. 22 and 23.

We have carefully checked the results obtained with the present description. For instance, if one assumes a uniform polarizability tensor ϵ, the reflectivity obtained should be equal to that directly obtained from the Fresnel relations. This is indeed the case.

To describe the appearance of the crystallite in the microscope, its optical spectrum was obtained by numerically integrating its Jones matrix across the solid angle covered by the objective lens, and multiplying the resulting integrated reflectivities with the Jones matrices of the polarizing optical components.

The integration was performed by choosing different azimuthal and polar angles of incidence on a grid of concentric circles, uniformly covering the solid angle cone of the objective lens. For each specific azimuthal incident direction, the polarization direction of the incident beam was accordingly expressed within the new reference frame by transformation (we neglect polarization changes induced by the lenses). The integration mesh was chosen sufficiently small that the resulting integral was independent of mesh size [the integrand (the Jones matrix) then only shows a small variation between the mesh points].

To enable comparison with the observed colors, the calculated light spectra were finally expressed in their corresponding red-green-blue (RGB) coordinates, as follows. The XYZ color coordinates were obtained from the spectra by integration using the XYZ color matching functions x_λ, y_λ, z_λ from the 1931 CIE colorimetric system $(\Delta\lambda = 5\ \text{nm})$.[24] The XYZ coordinates were finally converted into RGB intensities which correspond to the RGB chromaticity coordinates of the NTSC color television system.[25] The corresponding transformation is

$$\begin{aligned} \text{R} &= 1.753X - 0.489Y - 0.265Z, \\ \text{G} &= -0.998X + 2.027Y - 0.029Z, \\ \text{B} &= 0.070X - 0.141Y + 1.072Z, \end{aligned} \tag{2}$$

from which the perceived colors expressed in their RGB color coordinates are obtained.

C. Comparison with experiment

To test the predictions for the appearance of a single crystal in the microscope, we have recorded images from two α-$4T$ single crystals with thicknesses $\sim$160 nm and $\sim$200 nm, for different sample azimuths α_{sample} between 0° and 360°, both for ''linear'' and for ''circular'' light. The measured RGB color components[26] for the 157 nm crystallite as a function of sample azimuth are shown in Fig. 4 (circles).

The calculations (solid lines) show good agreement with all three observed RGB components, both for linear and cir-

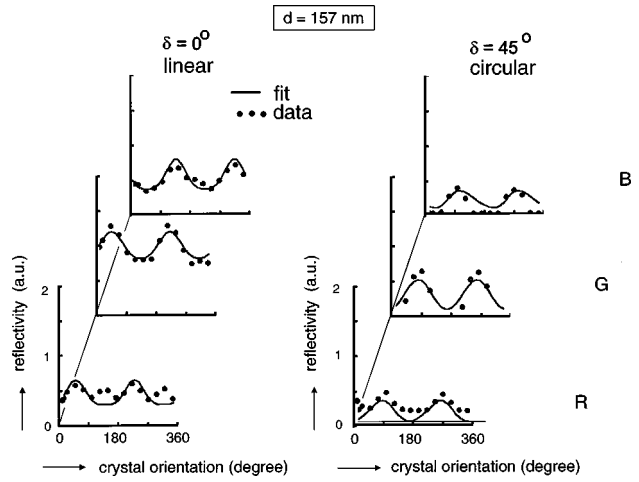

FIG. 4. Observed (circles) and calculated (lines) RGB coordinates of a single crystallite (thickness 157 nm) in the microscope. This particular crystallite shows green-blue color tones. The curves have been obtained assuming molecular polarizabilities of $\epsilon_{mol,11}=1.83$ and $\epsilon_{mol,22}=\epsilon_{mol,33}=4.04$.

cular incident polarization (Fig. 4). The fits for both crystallites have been simultaneously obtained, by varying the polarizabilities of the molecules (within the molecular plane the polarizabilities were assumed uniform, i.e., $\epsilon_{mol,22}=\epsilon_{mol,33}$), the film thickness, and the crystallite orientation χ_c within the film (so that $\alpha_c=\alpha_{sample}+\chi_c$), so as to obtain a good description of the data.

For both crystal structures I and II, the data are well described for $\epsilon_{mol,11}=1.83$ and $\epsilon_{mol,22}=\epsilon_{mol,33}=4.04$.[27] We note that with these molecular polarizabilities, waves under normal incidence encounter effective refractive indices of $n_b=1.84$ and $n_a=1.61$, as is found from the eigenvalues for these waves. This is in good agreement with the values obtained over macroscopic film areas (see Appendix B).

We have calculated the film colors for thicknesses between 0 and 600 nm and represented them in color charts (Fig. 5). By careful comparison with the colors observed, using a wafer with a large variation in thickness and large crystallites, we find that these charts match the observations

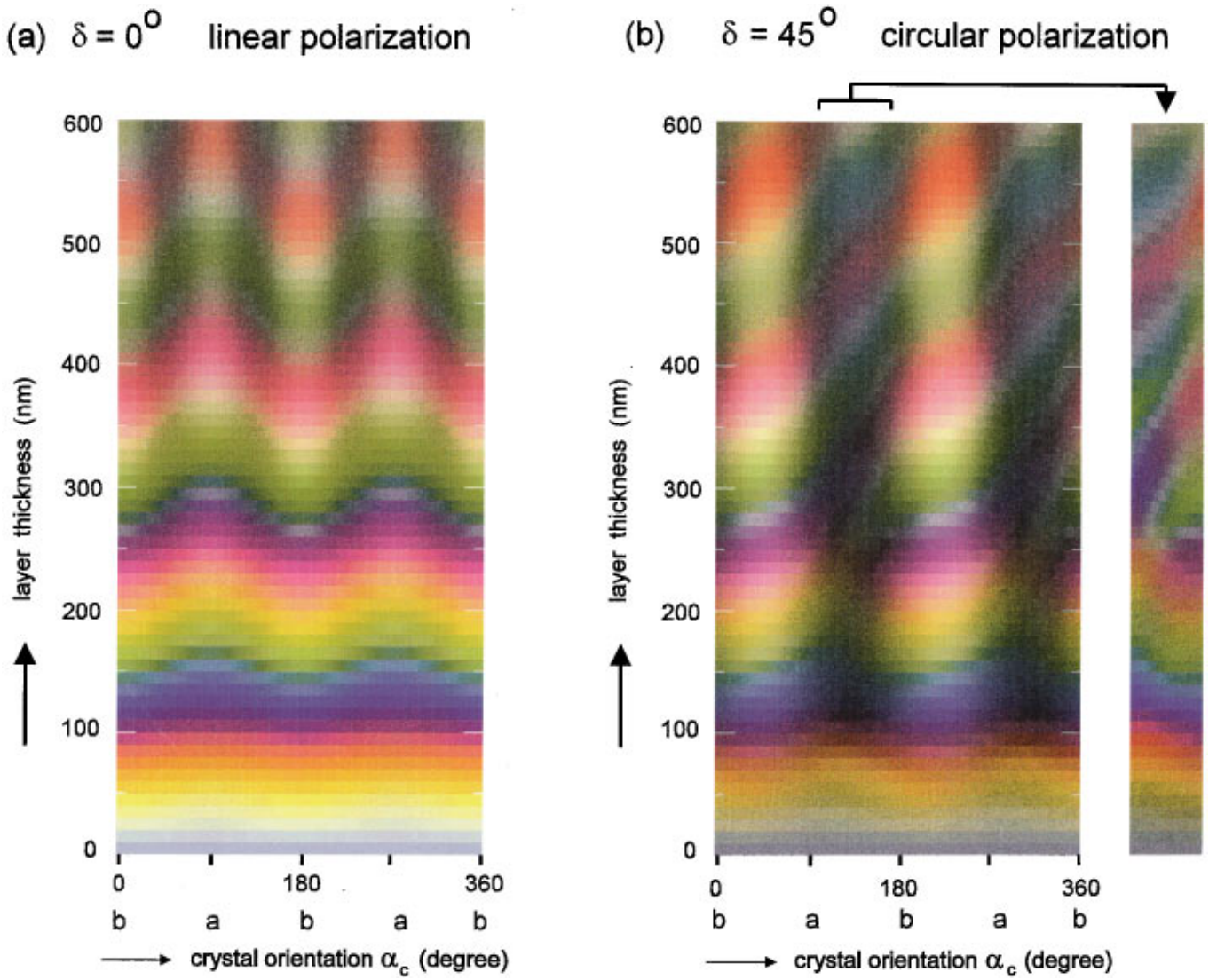

FIG. 5. (Color) Calculated colors of α-4T crystallites in the microscope. Colors are given for different crystal orientations and thicknesses, both for linear and circular polarization of the incident light, $\delta=0°$ and $\delta=45°$. Note that these charts are exclusively valid for a single SiO_2 film thickness and numerical aperture of the microscope objective lens. For this chart $d_{SiO_2}=161$ nm; $N.A._{objective}=0.9$.

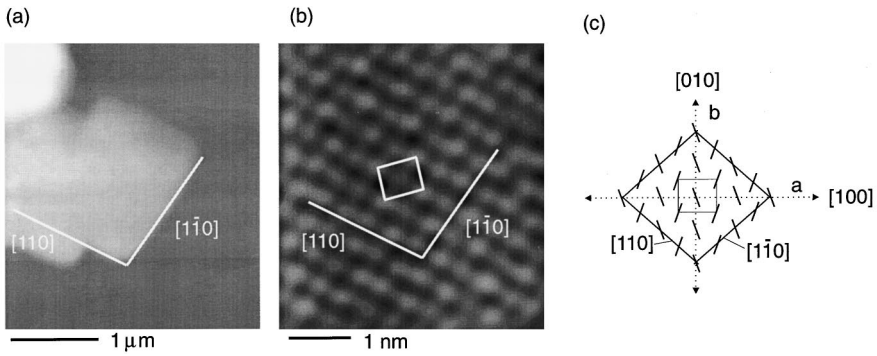

FIG. 6. AFM data confirming the assignments of the crystal axes. Large area scan (a) and scan zoomed in on the same island with molecular resolution (b) show that that the facet directions are $[1\bar{1}0]$ and [110] directions (c), in complete agreement with the optical data. These data provide conclusive evidence for the description given in this article.

in detail over the thickness range from 0 to 400 nm. For instance, consider the islands shown in Fig. 3 for $\delta=0°$. For a thickness of $\sim$200 nm, the ''yellow/red'' and ''greenish'' tones correspond to alignment of the *b* and the *a* crystal axes with the analyzer [see Fig. 5(a)]. The observations for circular light (Fig. 3, $\delta=45°$) also follow the calculation at 200 nm [Fig. 5(b)]: at $\alpha_c=45°$ a yellow colored maximum is found; the intensity almost vanishes at $\alpha_c=135°$. At $\alpha_c=0°$ and $\alpha_c=90°$ faint red and green tones are observed. For thicknesses between 0 and 400 nm, the thicknesses estimated from the chart agree within ± 10 nm with those measured by a profiler scan.

V. RECIPE FOR IDENTIFICATION OF THE *b* AND *a* AXES IN A CRYSTALLITE

The data discussed in Sec. IV provide an unequivocal criterion, which allows to identify the crystal axes in a simple recipe. The maximum in intensity observed for circular light, (i.e., $\delta=45°$) always occurs at $\alpha_c\sim+45°$, independent of thickness. A minimum is consistently found at $\alpha_c\sim135°$ [also represented in the separate vertical zone in Fig. 5(b)] for thicknesses up to $\sim$400 nm. The resulting recipe is described in Appendix A. It combines the criterion mentioned above with the color extremes occurring along the crystal axes ($\alpha_c=0°$ or $\alpha_c=90°$) for $\delta=0°$.

This recipe works well for crystallite thicknesses up to $\sim$400 nm. Beyond that thickness, a second maximum develops at $\alpha_c=135°$ with circular ($\delta=45°$) light [see Fig. 5(b)], and the ($\delta=45°$; $\alpha_c=45°$) criterion breaks down. Therefore, in order to identify the axes in this regime one has to rely on the precise color tones occurring. However, the ($\delta=0°$) color extremes still coincide with either the *a* or *b* axis, only their unequivocal identification becomes less straightforward: one runs the risk to mix up the *b* with the *a* axes for these large thicknesses.

VI. CONFIRMATION BY AFM

We finally note that the directions of the *b* and *a* crystal axes obtained agree with independent AFM measurements. The crystal orientation is reflected in the faceting shown by some of the α-4*T* crystallites. This faceting can be employed to check the relation between optical polarization and crystal microstructure, as the same facets are visible both in the optical microscope (Fig. 3) and in the AFM [Fig. 6(a)].

In the latter case, we have analyzed the surface crystal lattice on top of the same island by AFM in molecular resolution [Fig. 6(b)]. These data show the orientation of the unit cell, which has dimensions of 7.4 ± 1 and 8.4 ± 1 Å. The facets coincide with the [110] and [110] directions in the crystal [Fig. 6(c)]. Imaging the same crystallite in the polarization microscope, we find that the main optical axes bisect these facet directions, as expected. The *b* and *a* axes as determined in the optical experiment coincide with those found by AFM.

This completes the proof for the optical approach presented in this article.

VII. α-6*T*

First data on sexithiophene show that the approach presented here is directly applicable to this material as well. Films prepared at elevated substrate temperatures ($\sim$190 $\pm$40 °C) again show the well-known ensemble of six peaks in the x ray Θ-2Θ scans, indicative of the layered crystal structure, and crystallites with diameters of $\sim5-10$ μm.

The colors of these crystallites in the microscope show the same general behavior as a function of orientation in the microscope as quaterthiophene (Fig. 5). This shows that the method developed here generally applies to these materials.

VIII. DISCUSSION

A. Polarizability tensor

The results in this article are represented in terms of the in-plane refractive indices n_a and n_b, for the following reason. The main unknown optical parameter in this work is the optical polarizability of the organic crystal, as described by the general anisotropic tensor ϵ. The reflected colors, however, are almost completely determined by the polarizabilities within the surface plane, i.e., by effectively only two out of three tensor components.

This is true both for the appearance of the film in the microscope and to the eye. Specifically, the film color as apparent to the eye for light under normal incidence is expected to be completely independent of the out-of-plane op-

tical polarizability. On the other hand, the dependence of the colors in the microscope on the out-of-plane polarizabilities is also weak, as we find from our calculations. This is true even in the case of an objective with N.A.$\approx$1 (large magnification), where the light waves are incident on the sample with angles of incidence which deviate significantly from the normal direction.

Therefore, the out-of-surface-plane optical polarizabilities are not obtained from our experiments. Consequently, we specify the in-plane refractive indices n_a and n_b only. In practice the tensor used in the calculations has been constructed on the basis of either crystal structures I or II, assuming 'molecular' polarizabilities $(\epsilon_{\mathrm{mol}})_{ii}$, $(i=1,2,3)$, such that it reproduces the experimental data (see Sec. IV); n_a and n_b are found as the eigenvalues of the matrix Δ for normal wave incidence.

B. Wavelength dependence

Furthermore, we have neglected in our calculations a possible wavelength dependence of the polarizability. The polarizability is expected to vary especially around the main π-π^* absorption band ($\sim$580 nm). Nevertheless, the approach presented in this article appears to works well. The refractive indices n_a and n_b from the fits represent effective refractive indices, averaged over wavelength.

IX. CONCLUSIONS

A simple recipe allows to obtain the orientation and thickness of the individual organic single crystals in evaporated quaterthiophene films. The method is based on the optical birefringence of this material.

To establish the method, we have solved Maxwell's equations for plane waves in the anisotropic crystal. We obtain excellent agreement with the observed reflectances. The crystal shows biaxial anisotropy. The effective in-plane refractive indices are $n_b=1.84$ and $n_a=1.61$.

The directions of the a and b crystal axes as obtained from the optical experiment are fully confirmed by AFM with molecular resolution. The present method is easily extended to other materials.

ACKNOWLEDGMENTS

The authors thank K. van Hasselt, B. J. Hoenders, J. Knoester, and W. H. de Jeu for discussions. J. Wildeman and Syncom BV, Groningen, are acknowledged for materials synthesis. This work was supported by the Nederlandse Organisatie voor Wetenschappelijk Onderzoek (NWO) through the Stichting voor Fundamenteel Onderzoek der Materie (FOM).

APPENDIX A: RECIPE TO DETERMINE CRYSTAL AXES AND THICKNESS

(1) Bring the crystallite in the center of rotation of the rotatable sample stage. Rotating the crystallite in the microscope with crossed polarizers ($\delta=90°$), find those orientations where the reflected intensity vanishes. (This alignment can be performed with an accuracy of $\pm 3°$.)

Here either the a or the b axis of the crystallite coincides with the analyzer, $\alpha_c=90°$ or $\alpha_c=0°$.

(2) Identify the axes using circularly polarized incident light ($\delta=45°$).

(i) *b axis aligned with analyzer*, $\alpha_c=0°$. Rotating to positive or negative angles, the reflected intensity should increase or decrease [Fig. 5(b)]. This corresponds to approaching the maximum at $\alpha_c\approx 45°$, and the minimum at $\alpha_c\approx 315°$, respectively.

(ii) *a axis aligned with analyzer*, $\alpha_c=90°$. Now the opposite happens for rotation to positive or negative angles: the intensity will decrease or increase, respectively, approaching the minimum at $\alpha_c\approx 135°$, and the maximum at $\alpha_c\approx 45°$.

If the thickness is larger than $\sim$400 nm, a second maximum exists at $\alpha_c=135°/315°$. [See Fig. 5(b)]. In that case, the a and b axes cannot be distinguished.

(3) The crystallite thickness can be determined using Figs. 5(a) and 5(b) on the basis of the color extremes for $\alpha_c=0°$ and $\alpha_c=90°$ [$\delta=0°$, Fig. 5(a)] and $\alpha_c=45°$ and $\alpha_c=135°$ [$\delta=45°$, Fig. 5(c)]. A color chart corresponding to the specific SiO_2 thickness is required for this determination.

APPENDIX B: DETERMINATION OF REFRACTIVE INDICES FROM THE FILM APPEARANCE TO THE BARE EYE

The dependence of color on crystal thickness is already apparent upon inspection of the evaporated film by the bare eye. Such observations can be used to determine the effective refractive indices of the thiophene material for waves under normal incidence, as follows.

We have prepared two films with a large variation in thickness, on a clean nonoxidized Si(100) wafer, by putting them close to the α-4T source. The sample thicknesses have been measured using a Dektak surface profiler [Fig. 7(a)]. They are in good agreement with the well-known cosine angular flux distribution of the evaporation source.

On the basis of the measured thicknesses, we have calculated the optical reflectivity of the wafer for normal incidence [Fig. 7(b)]. The thickness distribution over the sample area is apparent in the observed interference colors. We have varied the refractive indices of the thiophene material in a calculation so as to reproduce the experimentally observed color pattern. We obtain agreement with the observed colors only if each of the microcrystals is assumed to be birefringent.[28] This is most evident with monochromatic light incident on the sample (see Fig. 8). The reflected intensity shows an oscillatory dependence on film thickness. However, the amplitude of the oscillation vanishes at a thickness of a few hundred nm. This behavior is expected for a birefringent crystal: for polarizations along the different optical axes a and b, different oscillation periods arise (Fig. 8). As a result, the total oscillation amplitude vanishes at a thickness characteristic for the two different refractive indices (Fig. 8). We find striking agreement between the calculated and observed colors, assuming that under normal incidence the light experiences in-plane effective refractive

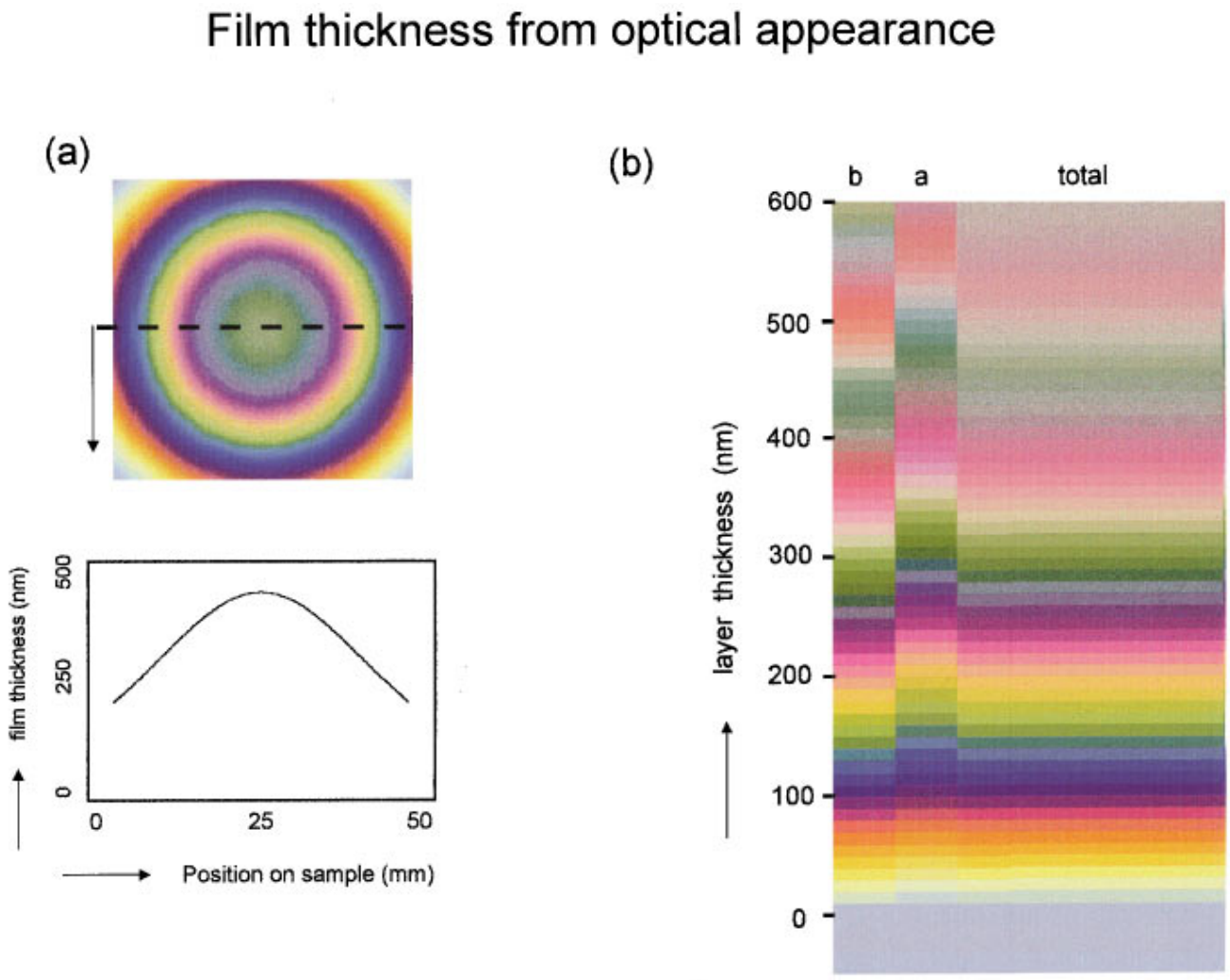

FIG. 7. (Color) Thickness-dependent color of an evaporated film to the naked eye. (a) Calculated appearance of a Si wafer with thicknesses between 435 nm (center) and 160 nm (border). The graph shows the thicknesses as measured by a Dektak profilometer. (b) Appearance as a function of thickness. This allows to estimate the thickness of a thin film on the basis of its color.

indices of $n_b = 1.83 \pm 0.03$ and $n_a = 1.63 \pm 0.03$, for polarization along the *b* and *a* axes, respectively. Having determined these parameters, the film thickness can be predicted from the observed color [Fig. 7(b)].

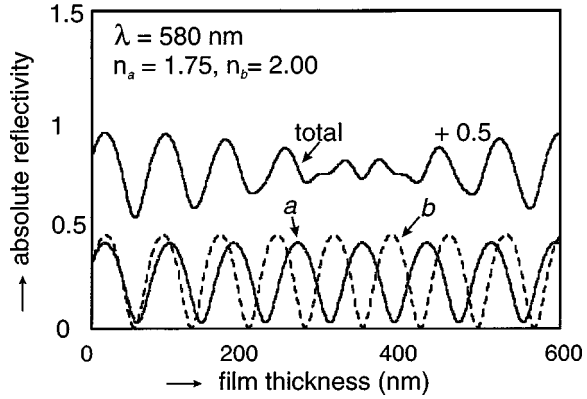

FIG. 8. Calculated reflectivities for monochromatic light of 580 nm under normal incidence, polarized along the *b* axis, along the *a* axis, and unpolarized ('total'). The oscillation as a function of thickness vanishes at a thickness of ~350 nm due to the difference in effective refractive index.

APPENDIX C: DISCRIMINATION OF CRYSTAL STRUCTURES I AND II

Observations in the microscope provide evidence in favor of crystal structure I (see Fig. 2). We observe an anomalous defocusing behavior for α-4T crystallites with crossed polarizers ($\alpha_c = 45°$, some intensity observed)—if the microscope is slightly defocused, each of the crystals shows an apparent translation in the image. This translation takes place along the direction of the *a* axis of that particular crystal.

We suggest that such a defocus-induced translation can be explained on the basis of the tilt in the optical axes that occurs for model I. The optical axes for models I and II do show a quite distinct difference in that respect. For model II, $\epsilon_{\text{crystal}}$ is diagonal in the unit cell frame. For model I, this is not the case. As a consequence, the optical axes are tilted with respect to the surface plane, and no longer coincide with the axis of the objective lens. Thus an asymmetry in the directions of ray propagation is introduced for model I.

Therefore, we believe that these data provide support for model I, in agreement with the powder diffraction data for α-4T by Porzio *et al.*[25]

[1] G. Horowitz, D. Fichou, X. Peng, Z. Xu, and F. Garnier, Solid State Commun. **72**, 381 (1989).
[2] K. Waragai, H. Akimichi, S. Hotta, H. Kano, and H. Sakaki, Phys. Rev. B **52**, 1786 (1995).
[3] A. Dodabalapur, H. E. Katz, L. Torsi, and R. C. Haddon, Science **269**, 1560 (1995).
[4] L. Torsi, A. Dodabalapur, L. J. Rothberg, A. W. P. Fung, and H. E. Katz, Science **272**, 1462 (1996).
[5] T. Holstein, Ann. Phys. (Paris) **8**, 343 (1959).
[6] A. J. Lovinger and L. J. Rothberg, J. Mater. Res. **11**, 1581 (1996).
[7] G. Horowitz, F. Garnier, A. Yassar, R. Hajlaoui, and F. Kouki, Adv. Mater. **8**, 52 (1996).
[8] W. A. Schoonveld, J. Vrijmoeth, and T. M. Klapwijk, unpublished results.
[9] *Crystals and the Polarizing Microscope*, 4th ed (Edward Arnold ltd., London, 1970).
[10] F. D. Bloss, *An Introduction to the Method of Optical Crystallography*, (Holt, Rinehart, and Winston, New York, 1962).
[11] P. A. Chollet, Thin Solid Films **68**, 13 (1980).
[12] L. Servant and M. J. Dignam, Thin Solid Films **242**, 21 (1994).
[13] For quaterthiophene, the polymorphism such as that reported for sexithiophene (see Ref. 16) is absent for the wide temperature range studied here.
[14] Crystals with diameters of $\sim 25\ \mu$m are formed for a substrate temperature of $76 \pm 10\ ^\circ$C and an evaporation rate of ~ 0.6 nm s^{-1}.
[15] W. Porzio, S. Destri, M. Mascherpa, and S. Brückner, Acta Polym. **44**, 266 (1993).
[16] B. Servet, G. Horowitz, S. Ries, O. Lagorsse, P. Alnot, A. Yassar, F. Deloffre, P. Srivastava, R. Hajlaoui, P. Lang, and F. Garnier, Chem. Mater. **6**, 1809 (1994).
[17] S. Hotta and K. Waragai, Adv. Mater. **5**, 896 (1993).
[18] F. van Bolhuis, H. Wijnberg, E. E. Havinga, E. W. Meijer, and E. G. J. Staring, Synth. Met. **30**, 381 (1989).
[19] The magnetic permeability μ is assumed unity.
[20] D. W. Berreman *et al.*, J. Opt. Soc. Am. **62**, 502 (1972); see also D. W. Berreman and T. J. Scheffer, Phys. Rev. Lett. **25**, 577 (1970).
[21] M. Born and E. Wolf, *Principles of Optics* 5th Ed. (Pergamon, New York, 1975).
[22] D. E. Aspnes and A. A. Studna, Phys. Rev. B **27**, 985 (1983).
[23] I. H. Malitson, J. Opt. Soc. Am. **55**, 1205 (1965).
[24] G. Wyszecki and W. S. Stiles, *Color Science* (Wiley, New York, 1966).
[25] J. Kamler, *Luminescent Screens*, 2nd Ed. (Iliffe Books, London, 1969).
[26] The experimental data have been obtained by integrating the reflected light over the same island area for each sample azimuth. This is realized by defining a circular area of integration in the digitized images.
[27] The polar angle of the molecules was taken 22°, the herringbone angle $\tau = 36°$. The film thicknesses obtained were 157 and 196 nm; the orientations $\chi_c = 80°$ and $\chi_c = 93°$, respectively.
[28] The crystals have a random azimuthal orientation with respect to the polarization of the light, as is evident from optical microscopy.